Bogoliubov Laboratory of Theoretical Physics

Theory of Nuclear Systems

- 2019—2023 → 2024 – 2030

Projects:

- Microscopic models for exotic nuclei and nuclear astrophysics
- Low-energy nuclear dynamics and properties of nuclear systems
- Quantum few-body systems
- Relativistic nuclear dynamics and nonlinear quantum processes

Publication activity: About 350 papers in the peer-reviewed journals for 5 years.

Scientific Staff

	Habilitation	PhD	No degree	Total
Nuclear Physics	27	24	9	60

49 – full-time positions
11 – half-time positions

Including: 3 PhD students
4 Students

Project:

Microscopic models for exotic nuclei and nuclear astrophysics

V.Voronov, A.Dzhioev

Nuclear Astrophysics

A.A. Dzhioev, K. Langanke, G. Martinez-Pinedo, A.I. Vdovin, Ch. Stoyanov

Unblocking of stellar electron capture rates for neutron-rich N = 50 nuclei at finite temperature

Phys. Rev. C 101 (2020) 025805

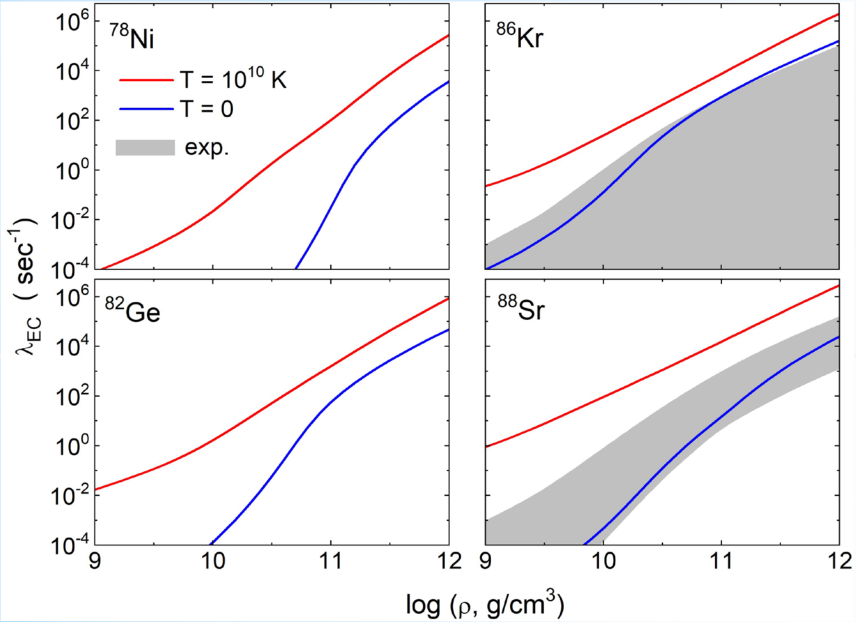

Electron capture rates as functions of core density during a supernova collapse.

Neutron-rich nuclei with N close to 50 are abundant in the core during a supernova collapse. The N = 50 shell gap could serve as an obstacle for electron captures in supernovae blocking GT transitions. **However, the finite-temperature calculations show that this blocking is overcome at finite temperatures due to thermal excitations.**

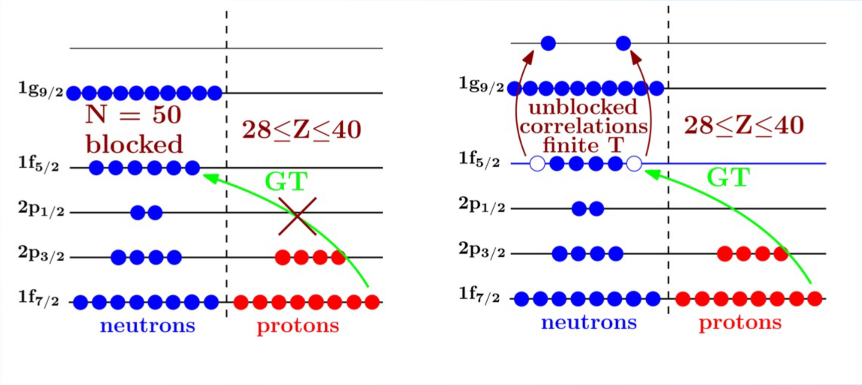

First calculation of the γγ -decay width of a nuclear 2^+_1 state: The case of ^{48}Ca

A. P. Severyukhin, N. N. Arsenyev, N. Pietralla, Phys. Rev. C **104**, 024310 (2021)

The γγ-decay reactions are formally analogous to neutrinoless double-β decay processes where in the latter two β-particles and in the former two γ-quanta appear in the final state and share the total transition energy.

Competitive γγ -decays open up new approaches to aspects of nuclear structure. The γγ / γ -decay of the low-energy quadrupole state of an even-even nucleus is studied. Choosing the first excited state of ^{48}Ca as an example, its γγ / γ branching ratio of 3×10^{-8} is computed for the first time for an even-even nucleus. This prediction can be tested experimentally. This work elucidates a new way to test our understanding of collective modes of nuclei and opens a perspective area of research.

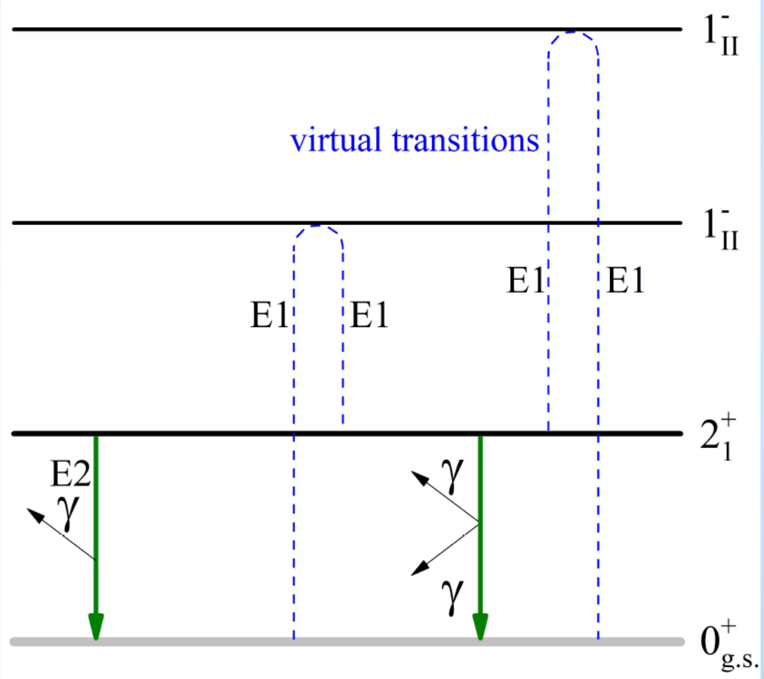

Two-state mixing scheme of the γγ-decay theory

$|1^-_I\rangle = \alpha|GR\rangle + \beta|GR\otimes 2^+_1\rangle$

$|1^-_{II}\rangle = -\beta|GR\rangle + \alpha|GR\otimes 2^+_1\rangle$

Physical Review C **103**, 044315 (2021)

Isoscalar monopole and dipole transitions in ^{24}Mg, ^{26}Mg, and ^{28}Si

P. Adsley ,V.O. Nesterenko, M. Kimura, L.M. Donaldson, R. Neveling, J. W. Brümmer, D. G. Jenkins, N.Y. Kheswa, J. Kvasil, K.C.W. Li, D. J. Marín-Lámbarri, Z. Mabika, P. Papka, L. Pellegri, V. Pesudo, B. Rebeiro, P.-G. Reinhard, F. D. Smit, and W. Yahia-Cherif

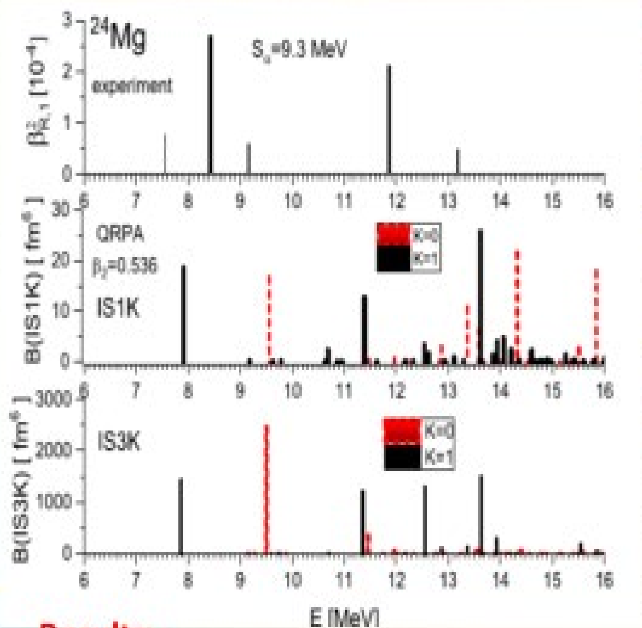

Experiment South Africa, iThemba, (a, a ′)
Theory: Skyrme QRPA (Dubna-Prague-Erlangen)
+ Antisym. Molecular Dynamics – AMD Japan

Background:

Two predictions: large isoscalar monopole (IS0) and dipole (IS1) transitions in light nuclei denotes clustering (AMD) or vortical modes (Skyrme QRPA).

Aim:

To check these predictions using new iThemba data for three very different nuclei:
prolate ^{24}Mg, soft ^{26}Mg and oblate ^{28}Si.

Results:

The states with large IS0 and IS1 strength in light nuclei have a complex nature combining cluster and mean-field (vorticity, IS0/IS2 and IS1/IS3 coupling,…) features This confirms cluster/mean-field duality of light nuclei. The low-energy vorticity is well localized in ^{24}Mg, fragmented in ^{26}Mg and almost absent in ^{28}Si.

Phys.Rev. C **105**, 024311 (2022)

Microscopic shell-model counterpart of the Bohr-Mottelson model

H. G. Ganev

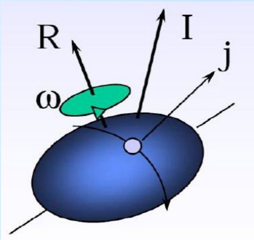

Two fundamental models of nuclear structure

1) **Bohr-Mottelson collective model** – Nobel Prize (1975);
2) **Shell Model** – Nobel Prize (1963);

The BM CM has proved to be very successful in describing the low-lying excitations in different nuclei with various collective properties (rotational, vibrational, transitional).

✓ How the BM collective dynamics is related to the more complete SM many-fermion dynamics?

$\Rightarrow$ The problem: giving the BM model a microscopic foundation!
(or embedding of the BM model in the SM)

❑ Solution: by algebraic approach

❑ Embedding:

1) In the one-component SM theory /G.Rosensteel and D.Rowe, Phys.Rev.Lett.38,10(1977)/

BM $\rightarrow$ Sp(6,R) model (rotations with vorticity + Giant Resonance vibrations;
no γ-unstable submodels of BM)

2) In the two-component proton-neutron SM theory

/H.G. Ganev, Eur.Phys.J.A57,181(2021)/

BM $\rightarrow$ PNSM with Sp(12,R) dynamical group, containing:

a) Sp(6,R) submodel

b) a large class of γ-unstable type submodels

EPJ A **58**, 182 (2022)

N.Yu. Shirikova, A.V. Sushkov, L.A. Malov, E.A. Kolganova, R.V.Jolos

Prediction of the excitation energies of the 2_1^+ states for superheavy nuclei based on the microscopically derived Grodzins relation [Phys. Rev. C105(2022) 024309]

Microscopically derived Grodzins relation and prediction of the excitation energies of the 2_1^+ states for some superheavy nuclei [Phys. Part. Nucl. 53(2022) 1138]

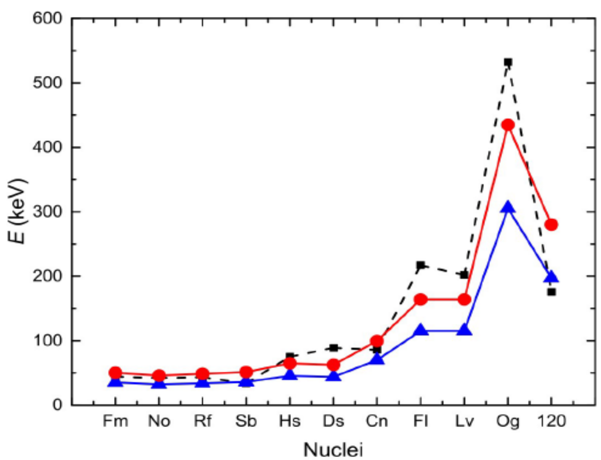

FIG. 2. The predicted energies of the 2_1^+ states for different nuclei. Calculations are performed for the microscopic variant of the Grodzins relation (17) (variant [A]) and the phenomenological Grodzins relation (1) [$E(2_1^+)_{\max}$ and $E(2_1^+)_{\min}$ with the proportionality coefficient 3.02 and 2.12, respectively]. Solid line with circles (red): $E(2_1^+)_{\max}$; solid line with triangles (blue): $E(2_1^+)_{\min}$; dashed line with squares (black): variant [A].

Based on the phenomenological

$$E(2_1^+) \times B(E2; 0_1^+ \to 2_1^+) = 2.57(\pm 45) Z^2 A^{-2/3}$$

and microscopical Grodzins relation

$$E(2_1^+) \times B(E2; 0_1^+ \to 2_1^+) = \hbar^2 q^2 \langle 0_1^+ | (B^{-1})_{00} | 0_1^+ \rangle$$

derived using the Bohr collective Hamiltonian and the Quasiparticle-Phonon nuclear model, the excitation energy of the first 2_1^+ states of the chain of even-even superheavy nuclei with Z from 100 to 120 are predicted. Calculations are performed for several sets of deformation parameter β_2 calculated by using the Strutinsky method or taken from the other publications. It is found that for all sets of deformation parameters, at the beginning of the studied region of nuclei at $Z = 100 - 110$, where quadrupole deformation is large, the energies of the 2_1^+ states do not exceed 100 keV, i.e., correspond to rotational states. Then, with decrease in deformation, $E(2_1^+)$ rises sharply and reaches a maximum value in ^{284}Fl or in ^{292}Og, i.e., in nuclei with minimal values of β_2.

R.V.Jolos, E.A.Kolganova, Phys. Lett. B 820, 136581 (2021)

Project:

Low-energy nuclear dynamics and properties of nuclear systems

S.Ershov, N.Antonenko

E. V. Mardyban, E. A. Kolganova, T. M. Shneidman, R. V. Jolos

“Evolution of the phenomenologically determined collective potential along the chain of Zr isotopes”

Phys. Rev. C105 (2022) 024321

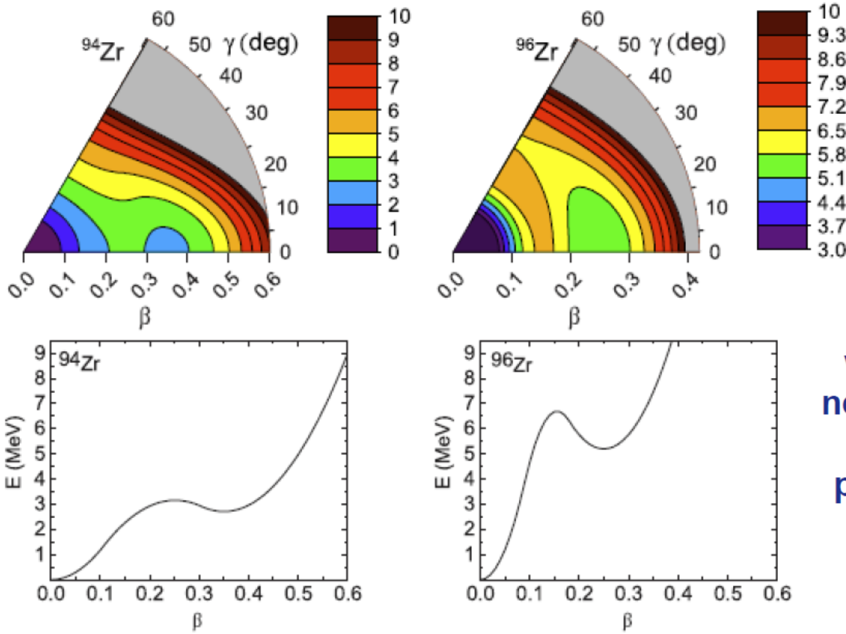

Collective potential for the even-even Zr isotopes obtained by fitting the experimental data for low-lying collective quadrupole states.

Purpose:

To investigate the properties of the low-lying collective states of $^{92-102}Zr$ based on the five-dimensional Bohr collective hamiltonian.

The relative depth of two minima, height and width of the barrier, and rigidity of the potential near both minima are determined so as to achieve the best possible description of the observed properties of the low-lying collective quadrupole states.

The low-energy structure of $^{92-102}Zr$ can be described in a satisfactory way

Ma.von Tresckow, M.Rudigier, T.M.Shneidman et al.

“New evidence for alpha clustering structure in the ground state band of ^{212}Po”

Phys. Lett. B821 (2021) 136624

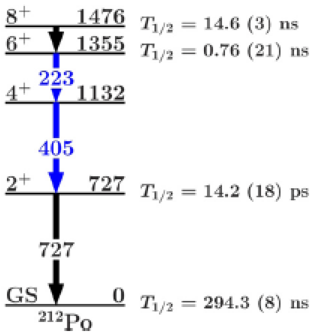

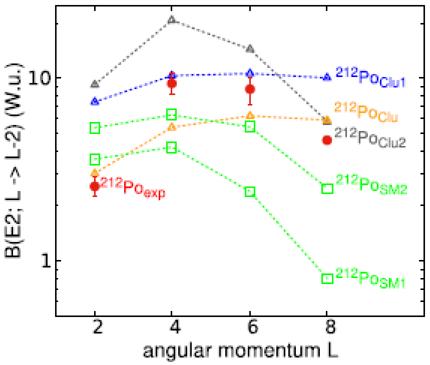

Half-lives of the low-lying yrast states of ^{212}Po have been measured using the delayed coincidence fast-timing method.

The first measurement of the 4_1^+ half-life, and a new measurement of the 6_1^+ half-life with improved accuracy compared to previous studies is reported.

Comparison of the new available data with an α-clustering model calculation provides evidence that the inclusion of the α-cluster degree of freedom significantly improves agreement with experimental data compared to earlier shell model calculations.

This suggests that α-cluster components play an important role in the structures of these states.

T.M. Shneidman, N. Minkov, G.G. Adamian, N.V. Antonenko

"Effect of Coriolis mixing on lifetime of isomeric states in heavy nuclei"

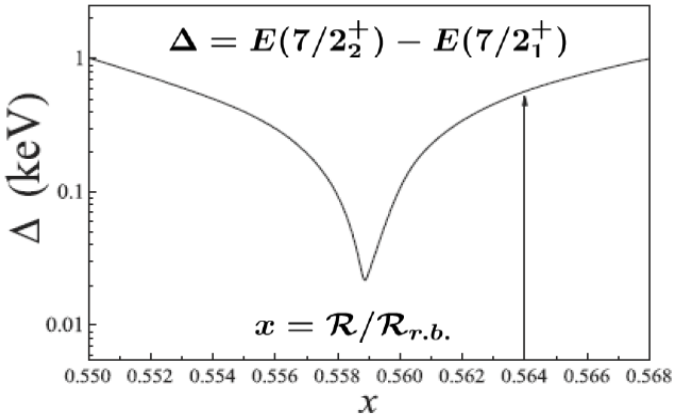

Phys. Rev. C106 (2022) 014310

The effect of Coriolis K mixing on the γ decay of one-quasiparticle isomeric states is examined in transfermium nuclei with N = 153.

Assumption: Coriolis interaction can produce the strong enhancement of the decay rates of isomeric states due to accidental degeneracy with the rotational states built on nonisomeric structures.

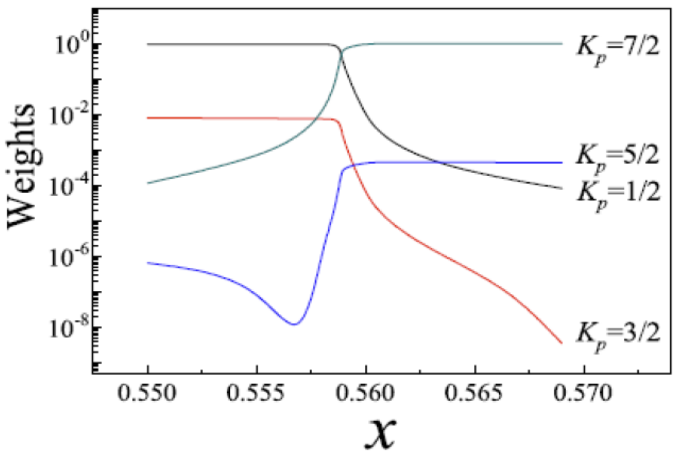

This mechanism is likely to explain the 38-ns $K^\pi = 7/2^+$ isomer in ^{251}Cf which is quasidegenerated with an $I = 7/2^+$ rotation state built on $K^\pi = 1/2^+$.

Model explains the enhancement of its decay by three orders of magnitude compared to the $K^\pi = 7/2^+$ isomer in ^{249}Cm.

A. Rahmatinejad, T. M. Shneidman , G. Adamian, N. V. Antonenko,
B. P. Jachimowicz, M. Kowal

“Energy dependent ratios of level-density parameters in superheavy nuclei”

Phys. Rev. C105 (2022) 044328

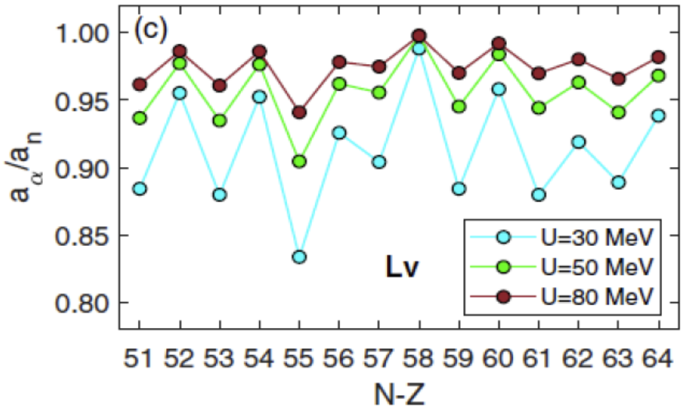

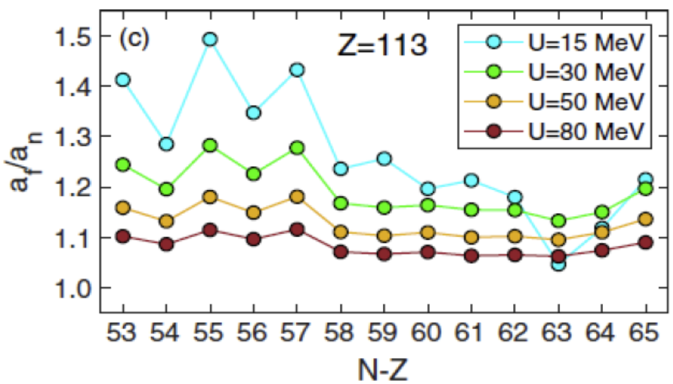

The intrinsic level densities of SHN with Z = 112 – 120 at the ground state and at the saddle point are calculated within the thermodynamic superfluid formalism.

The single-particle energies, shell corrections and nuclear masses were obtained within the multidimensional microscopic-macroscopic model. Spectra were generated at global minima of the adiabatic potential energy surfaces.

The level-density parameter ratios increase with excitation energy and reach an asymptotic value less than 1.1 for a_f/a_n and less then unity for $a_{p,\alpha}/a_n$.

In the case of α decay the collective enhancement caused by cluster degrees of freedom were identified.

A.N. Bezbakh, G.G. Adamian, N.V. Antonenko

“Role of spin-orbit strength in the prediction of closed shells in superheavy nuclei”

Phys. Rev. C105 (2022) 054305

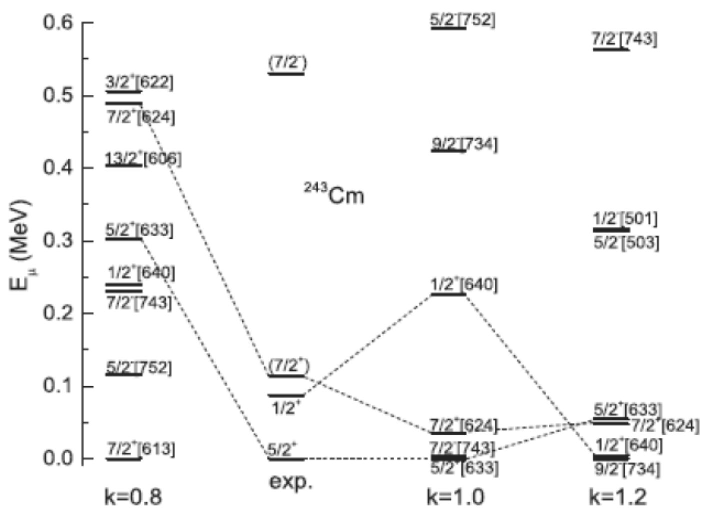

Unsolved controversy:

- ❑ microscopic-macroscopic approaches locate the proton shell closure at flerovium (Fl, Z = 114)
- ❑ the nonrelativistic and relativistic self-consistent approaches predict stronger shel effects at Z = 120 - 126

The strength of the spin-orbit interaction is crucial to define the position of the shell closures in nuclei beyond lead. The 20% variation of the spin-orbit strength can strongly shift the position of the minimum E_{sh}

Spectra of low-lying one-quasineutron states are compared with the available experimental data. The parameters of the TCSM were set at k = 1 for the best description of the experimental one-quasiparticle spectra.

With decreasing spin-orbit strength (k = 0.8) the proton shell closure is shifted to Z = 126. For larger spin-orbit interaction (k = 1.2), the nuclei with Z = 114 are calculated to have the largest value of shell-correction energy.

L. A. Malov, G. G. Adamian, N. V. Antonenko, H. Lenske

"Shaping the archipelago of stability by the competition of proton and neutron shell closures"

Phys. Rev. C 104 (2021) L011304

Evolution of superheavy nuclei in proton and neutron number is explored by investigating the ground-state shell correction energy in the Z = 112 - 126 and N = 170 - 190 region

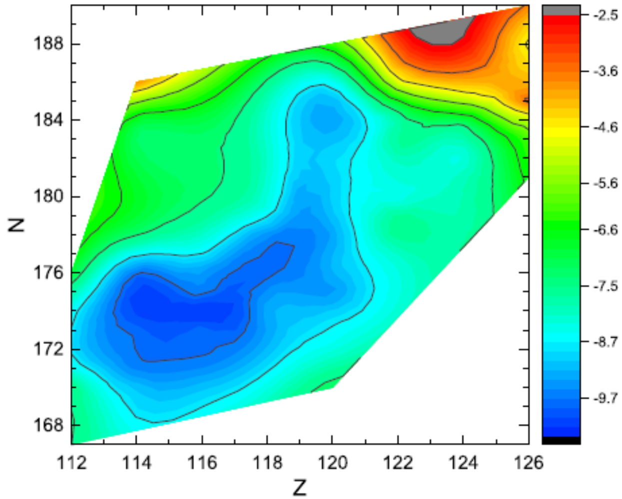

ground-state shell correction energy

A new approach:

incorporate into the microscopic-macroscopic approach potentials derived self-consistently by EDF + HFB theory

Central result: the strong influence of the neutron shell structure on the evolution of SHN (obtained for the first time)

Instead of an island of stability it is discovered a landscape of a hilly ridge on a coral reef formed by the competition of proton and neutron shell closures at Z = 114 and Z = 120, and N = 174 and N = 184

^{288}Fl is predicted as the next double magic nucleus after ^{208}Pb

Juhee Hong, G. G. Adamian, N. V. Antonenko, M. Kowal, P. Jachimowicz

Isthmus connecting mainland and island of stability of superheavy nuclei

Phys. Rev. C 106, 014614 (2022)

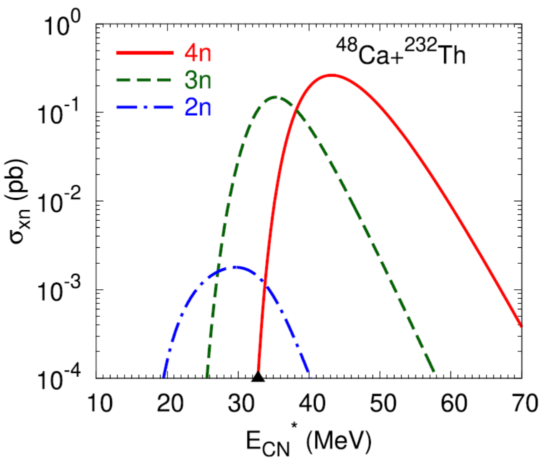

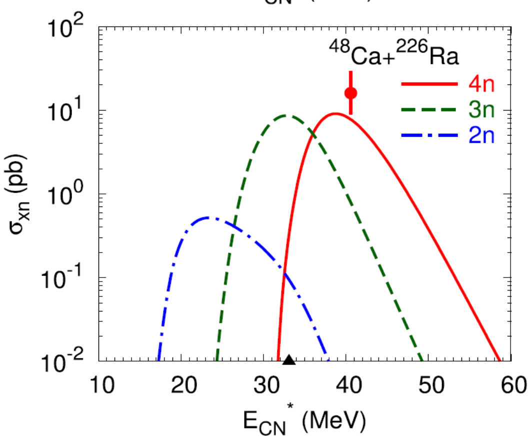

For the ^{48}Ca +^{232}Th → ^{277}Ds+3n reaction, we predict a maximum cross section $\sigma_{3n} \approx 0.1$ pb, which is smaller than the experimental production cross sections in the ^{48}Ca +^{226}Ra → ^{270}Hs+4n reaction and $\sigma_{3n} \approx 3, 10, 3$ pb in the reactions ^{48}Ca+^{238}U → ^{283}Cn+3n, ^{48}Ca+^{242,244}Pu → ^{287,289}Fl+3n, ^{48}Ca+^{245,248}Cm → ^{290,293}Lv+3n, respectively. The nucleus with Z = 110 seems to be the boundary nucleus between the mainland (where the last nucleus is Hs) and the island (archipelago) of stability of superheavy nuclei. In other words, the Ds nucleus is located at the isthmus connecting the island of stability and the mainland from the side of a relatively neutron-rich nuclei.

The production cross section on the atomic number *Z* from Hs to Lv has a minimum in the Ds nucleus.

Hot and cold fusion reactions leading to the same superheavy evaporation residue

Eur. Phys. J. A (2022) 58:180

Employing the ^{48}Ca+^{233}U reaction in the 4*n*-evaporation channel, one can directly produce the ^{277}Cn isotope, which was previously synthesized in the 1*n*-evaporation channel of the cold fusion reaction ^{70}Zn+^{208}Pb. The production cross sections are comparable within the experimental and theoretical uncertainties.

I.S. Rogov, G.G. Adamian, N.V. Antonenko

“Cluster approach to spontaneous fission of even-even isotopes of U, Pu, Cm, Cf, Fm, No, Rf, Sg, and Hs”

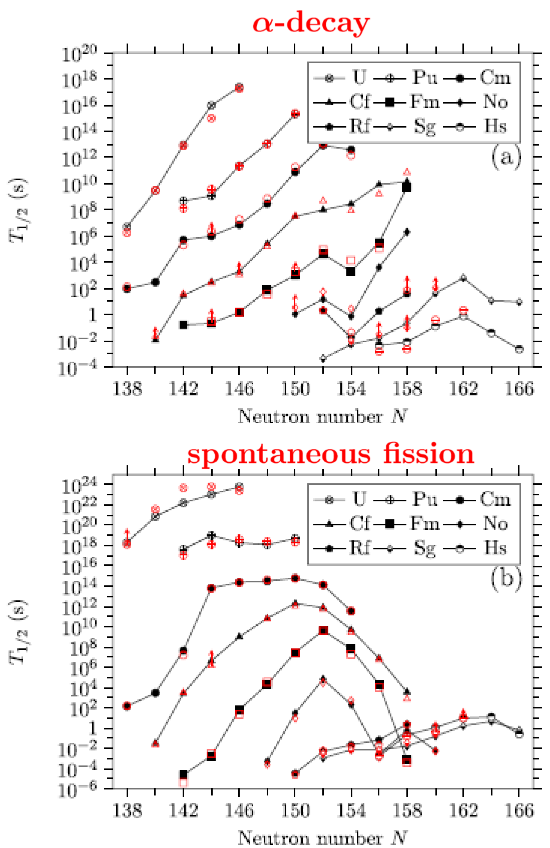

Phys. Rev. C 104 (2021) 034618

For even isotopes of nuclei U, Pu, Cm, Cf, Fm, No, Rf, Sg, and Hs, spontaneous fission and α-decay half-lives are calculated within the dinuclear system model and compared with existing experimental data.

Cluster radioactivity half-lives are also described for even U, Pu, and Cm isotopes.

All processes are considered for the evolution of a nucleus in the charge (mass) asymmetry coordinate and in the relative distance between the centers of clusters formed.

In contrast to the existing fission models, model gives correct absolute values for $T_{1/2}$ of spontaneous fission, cluster radioactivity, and α-decay.

In terms of spontaneous fission (α-decay) half-lives, the model presented describes well the values, which differ up to 34 (20) orders of magnitude. Larger values of spontaneous fission half-lives at N = 152 are well described.

Phys. Rev. C **105** (2022) 034619

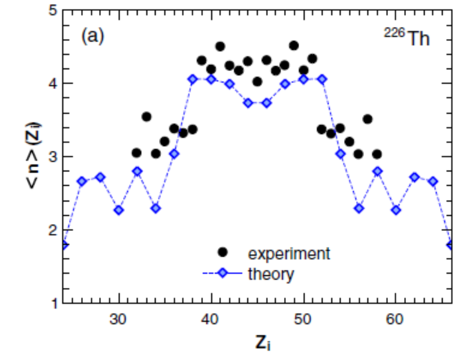

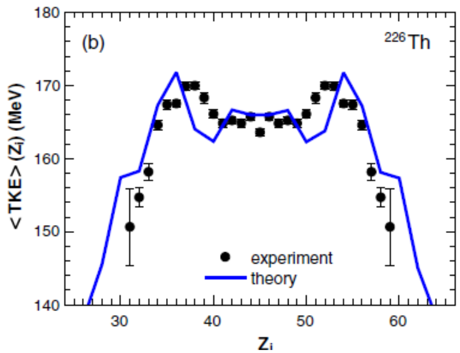

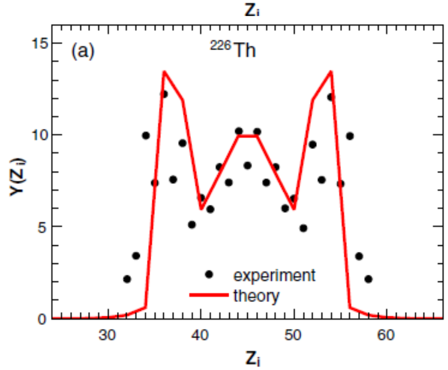

H. Pasca, A. V. Andreev, G. G. Adamian, N. V. Antonenko

"Simultaneous description of charge, mass, total kinetic energy, and neutron multiplicity distributions in fission of Th and U isotopes"

Phys. Rev. C 104 (2021) 014604

For fissioning isotopes of thorium and uranium, simultaneous description of charge, mass, total kinetic energy, and neutron multiplicity distributions of fission fragments is presented within the improved scission-point model. Correlations between all these observables are analyzed. The influence of transition from symmetric to asymmetric fission mode on the shape of neutron multiplicity distribution is studied.

The most important step of the scission-point model is calculation of the potential energy of the dinuclear system as a function of charge Z_i, mass A_i, deformations β_i of two fragments, and internuclear distance R between them.

$$U = U_L^{LD} + \delta U_L^{shell} + U_H^{LD} + \delta U_H^{shell} + V^C + V^N$$

The improved scission-point model of fission is able to consistently and reliably describe several fission observables for fissioning nuclei ^{222,226,230}Th and ^{230,234}U at an average excitation energy $E^* = 11$ MeV.

V. V. Sargsyan, G. G. Adamian, N. V. Antonenko, H. Lenske

"Constraints on the appearance of a maximum in astrophysical S-factor"

Phys. Lett. B824 (2022) 136792

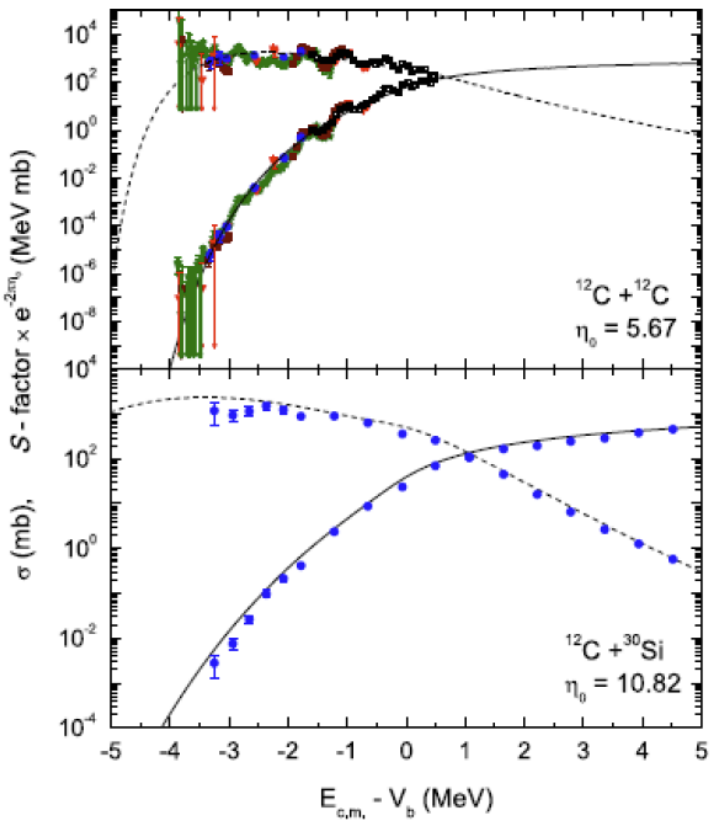

The calculated fusion excitation function and astrophysical S-factor

The structure of astrophysical S-factor for various reactions is analyzed within the extended quantum diffusion approach.

The calculated fusion cross sections are compared with the available experimental data. A good descriptions of the experiments have been obtained in all cases.

For the considered reactions, the S-factor shows a clear maximum in the sub-barrier energy range
$E_s \sim (0.60 – 0.86)\ V_b$

An analytical expression, predicting the dependence of the S-factor maximum on the ion mass and charge numbers, have been proposed.

S. N. Ershov, S. A. Rakityansky

"Jost matrices for some analytically solvable potential models" Phys. Rev. C 103 (2021) 024612

The S-matrix is a multivalued matrix function of the complex energy-variable E.
This means that a single value of E corresponds to several
(or even infinite in the case of Coulomb forces) different values of S(E).
S-matrix is defined not on the single E plane, but on a multilayered Riemann surface.

A family of analytically solvable potential models
for the one- and two-channel problems
is developed within the Jost matrix approach.
The potentials are chosen to be constant
in the interior region and to have different asymptotic
behavior (tails) at large distances.

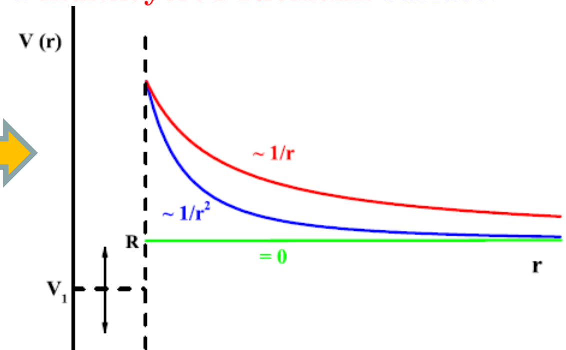

The migration of the S-matrix poles on the Riemann surface
of the energy, caused by variations of the potential strength,
is studied. It is demonstrated that the long-range ($\sim 1/r^2$)
tails and Coulomb potential (1/r) cause an unusual behavior
of the S-matrix poles. The Coulomb tail not only changes
the topology of the Riemann surface, but also breaks down
the so-called mirror symmetry of the poles in both
the single-channel and the two-channel problems.

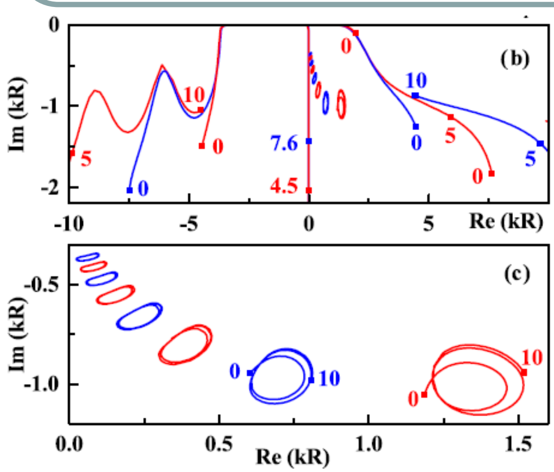

T.J. Tshipi, S. A. Rakityansky, S. N. Ershov

“Resonant states 3^+ and 2^- of the Boron isotope ^8B"

Int. J. Mod. Phys. E31 (2022) 225(

The Jost functions, constructed by fitting available partial cross-sections for the elastic p ^{7}Be scattering with $J^\pi = 3^+, 2^-$, are analytically continued to complex energies, where the resonances are located as their zeros. In addition to the resonance energies and widths, the residues of the S-matrix at the corresponding poles, as well as the Asymptotic Normalization Constants (ANC) are determined. The fitting is done using the semi-analytic representation of the Jost function with proper analytic structure, defined on the Riemann surface whose topology involves not only the square-root but also the logarithmic branching caused by the Coulomb interaction.

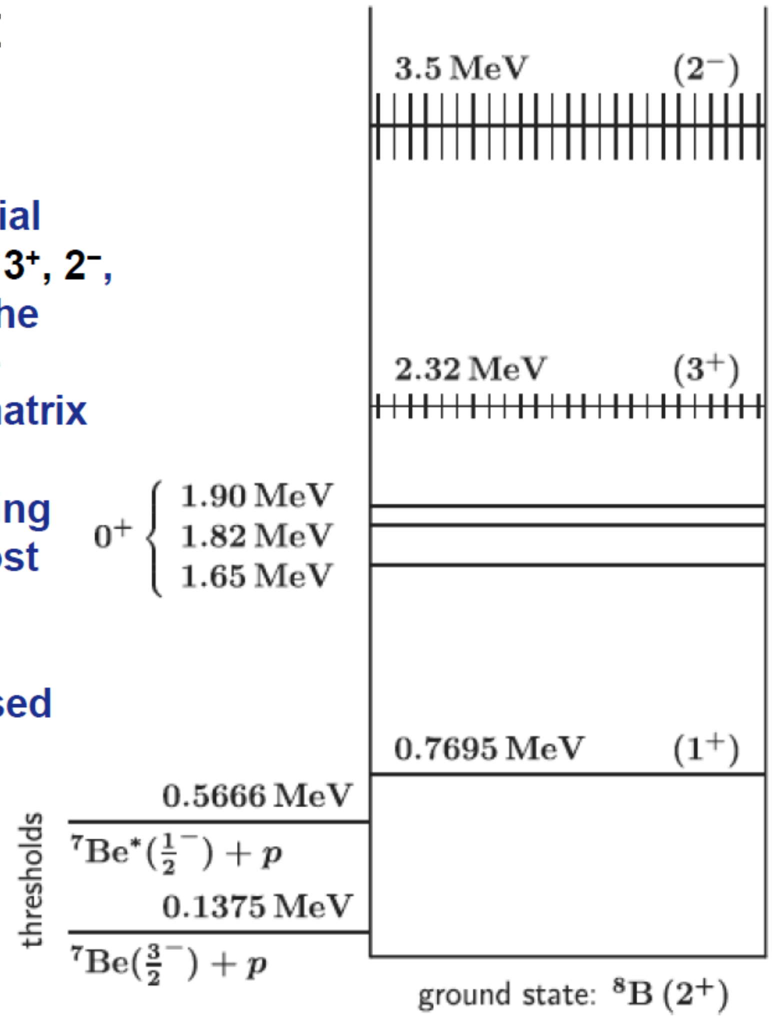

РОССИЙСКАЯ ФЕДЕРАЦИЯ

(19) **RU** (11) **210 191** (13) **U1**

(51) МПК
F24S 90/00 (2018.01)
H02S 10/30 (2014.01)

ФЕДЕРАЛЬНАЯ СЛУЖБА
ПО ИНТЕЛЛЕКТУАЛЬНОЙ СОБСТВЕННОСТИ

(12) ОПИСАНИЕ ПОЛЕЗНОЙ МОДЕЛИ К ПАТЕНТУ

(52) СПК
F24S 90/00 (2021.02); H02S 10/30 (2021.02)

(21)(22) Заявка: 2020143528, 28.12.2020

(24) Дата начала отсчета срока действия патента:
28.12.2020

Дата регистрации:
31.03.2022

Приоритет(ы):
(22) Дата подачи заявки: 28.12.2020

(45) Опубликовано: 31.03.2022 Бюл. № 10

Адрес для переписки:
141982, Московская обл., г. Дубна, ул. Университетская, 19, ФГБОУ ВО "Университет "Дубна"

(72) Автор(ы):
Моржухин Артём Маркович (RU),
Моржухина Светлана Владимировна (RU),
Назмитдинов Рашид Гиясович (RU),
Гладышев Павел Павлович (RU)

(73) Патентообладатель(и):
Государственное бюджетное образовательное учреждение высшего образования Московской области "Университет "Дубна" (государственный университет "Дубна") (RU)

(56) Список документов, цитированных в отчете о поиске: RU 2643262 C2, 31.01.2018. RU 2460863 C2, 10.09.2012. RU 2111422 C1, 20.05.1998. KZ 26293 A4, 15.10.2012. GB 2471844 A, 19.01.2011.

RU 210191 U1

(54) СОЛНЕЧНЫЙ ТЕПЛОВОЙ КОЛЛЕКТОР ДЛЯ ОТВОДА ТЕПЛА ОТ СОЛНЕЧНОЙ ФОТОВОЛЬТАИЧЕСКОЙ ПАНЕЛИ

(57) Реферат:
Полезная модель относится к области энергосбережения и может использоваться для увеличения эффективности солнечной панели за счет отвода излишнего тепла в ходе выработки электроэнергии, при необходимости к тепловому аккумулятору. Солнечный тепловой коллектор для отвода тепла от солнечной фотовольтаической панели содержит параллельные каналы для прохода теплоносителя, вход и выход теплоносителя. Корпус коллектора выполнен из теплоизоляционного материала, а роль крышки корпуса коллектора выполняет горячая поверхность электрической солнечной панели, прилегающая к параллельным каналам с теплоносителем. Избыточное тепло возможно применять для нагрева воды, либо для других сфер, например, для сушки и т.д. Солнечный тепловой коллектор для сбора излишнего тепла предлагает экономичное, компактное и эффективное решение для повышения эффективности солнечной панели и производства тепла для последующего использования. 2 ил.

RU 210191 U1

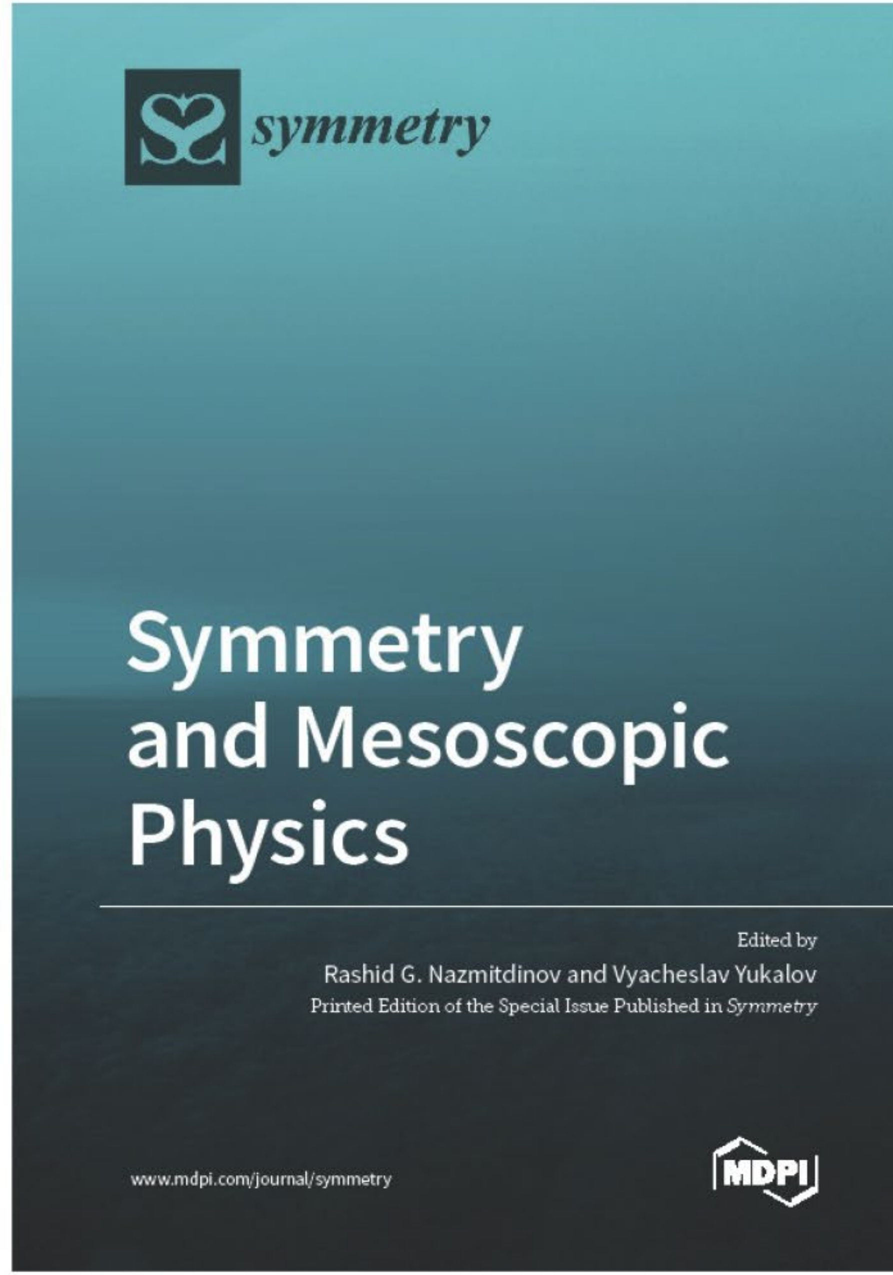

Project:

Quantum few-body system

A.Motovilov, V.Melezhik

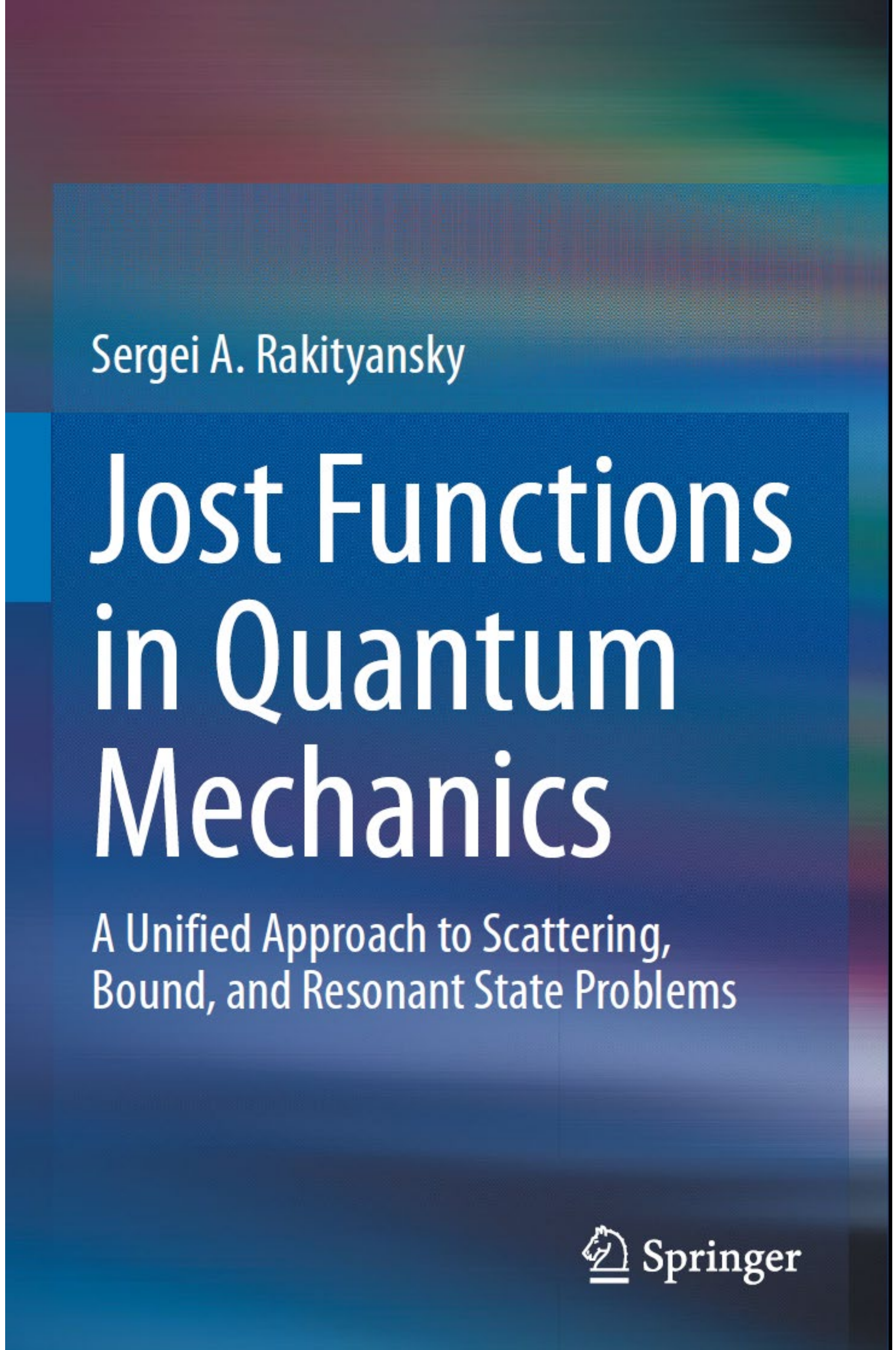
Sergei A. Rakityansky
Jost Functions in Quantum Mechanics
A Unified Approach to Scattering, Bound, and Resonant State Problems
Springer

2022

Eur. Phys. J. A (2022) 58:34
https://doi.org/10.1140/epja/s10050-022-00684-z
THE EUROPEAN PHYSICAL JOURNAL A

Investigation of low-lying resonances in breakup of halo nuclei within the time-dependent approach

Dinara Valiolda[1,2,3], Daniyar Janseitov[1,2,3,a], Vladimir Melezhik[3,4,b]

[1] Al-Farabi Kazakh National University, al-Farabi St. 74, Almaty, Republic of Kazakhstan
[2] Institute of Nuclear Physics, Ibragimova St. 1, Almaty, Republic of Kazakhstan
[3] Bogoliubov Laboratory of Theoretical Physics, Joint Institute for Nuclear Research, Joliot-Curie St. 6, Dubna, Russian Federation

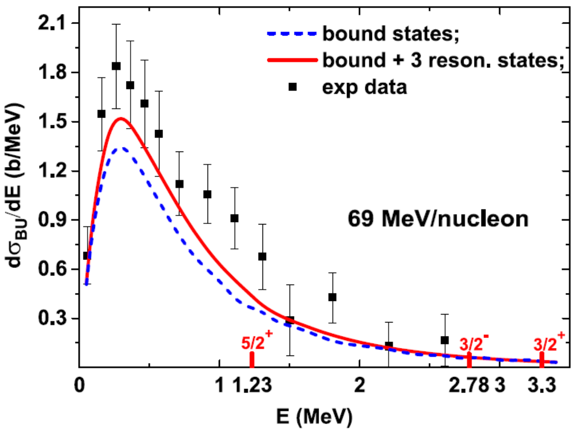

We performed calculations with quantum-quasiclassical approach in which relative dynamics of a neutron with respect ^{10}Be is described by the 3D Schrödinger equation $i\hbar\frac{\partial}{\partial t}\Psi(\mathbf{r},t) = H(\mathbf{r},t)\Psi(\mathbf{r},t)$ integrated simultaneously with the Hamilton equations $\frac{d}{dt}\mathbf{P} = -\frac{\partial}{\partial \mathbf{R}}H_{BP}(\mathbf{P},\mathbf{R},t)$, $\frac{d}{dt}\mathbf{R} = \frac{\partial}{\partial \mathbf{P}}H_{BP}(\mathbf{P},\mathbf{R},t)$, which describe the relative Be – Pb motion. It includes the projectile deformation and the energy transfer between the target and projectile.

^{11}Be + ^{208}Pb $\rightarrow$ ^{10}Be + n + ^{208}Pb

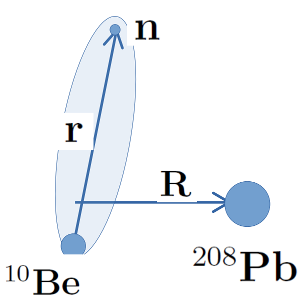

Our calculations are so far the only ones in the region around 10 MeV/nucleon, which is of great interest, since this is the energy range of HIE-ISOLD at CERN and the future ReA12 at MSU

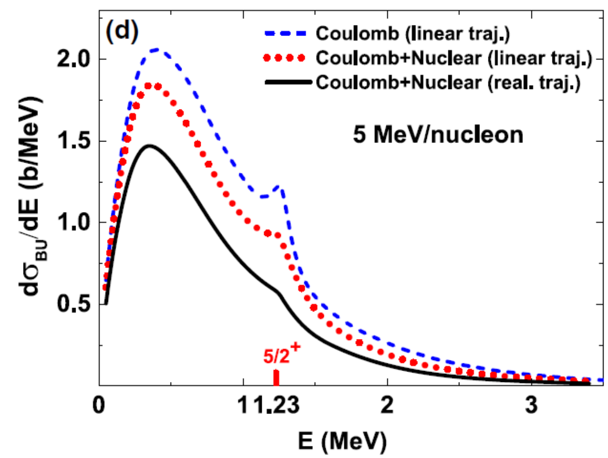

O. Chuluunbaatar[1], A.A. Gusev[1], S.I. Vinitsky[2] and A.G. Abrashkevich[3], P.W. Wen[4], C.J. Lin[5], KANTBP 3.1: A program for computing energy levels, reflection and transmission matrices, and corresponding wave functions in the coupled-channel and adiabatic approaches,
Compput. Phys. Commun. 278, pp. 108397–1–14 (2022).
[1]MLIT, JINR, [2]BLTP, JINR,[3]IBM Toronto Lab, Canada, [4]CIAE, Beijing,China, [5]GNU, Guilin,China

A FORTRAN program for calculating energy values, reflection and transmission matrices, and corresponding wave functions in a coupled-channel approximation of the adiabatic approach is elaborated and published in CPC Program Library.

Results of benchmark calculations for the fusion cross sections of ^{36}S+^{48}Ca, ^{64}Ni+^{100}Mo reactions are presented in figures. KANTBP 3.1 calculations show a good agreement with experimental data in the both low, medium and high energy. CCFULL calculations [CPC 123 (1999) 143 and its modification (2010))] show a good agreement with experimental data only in medium energy.

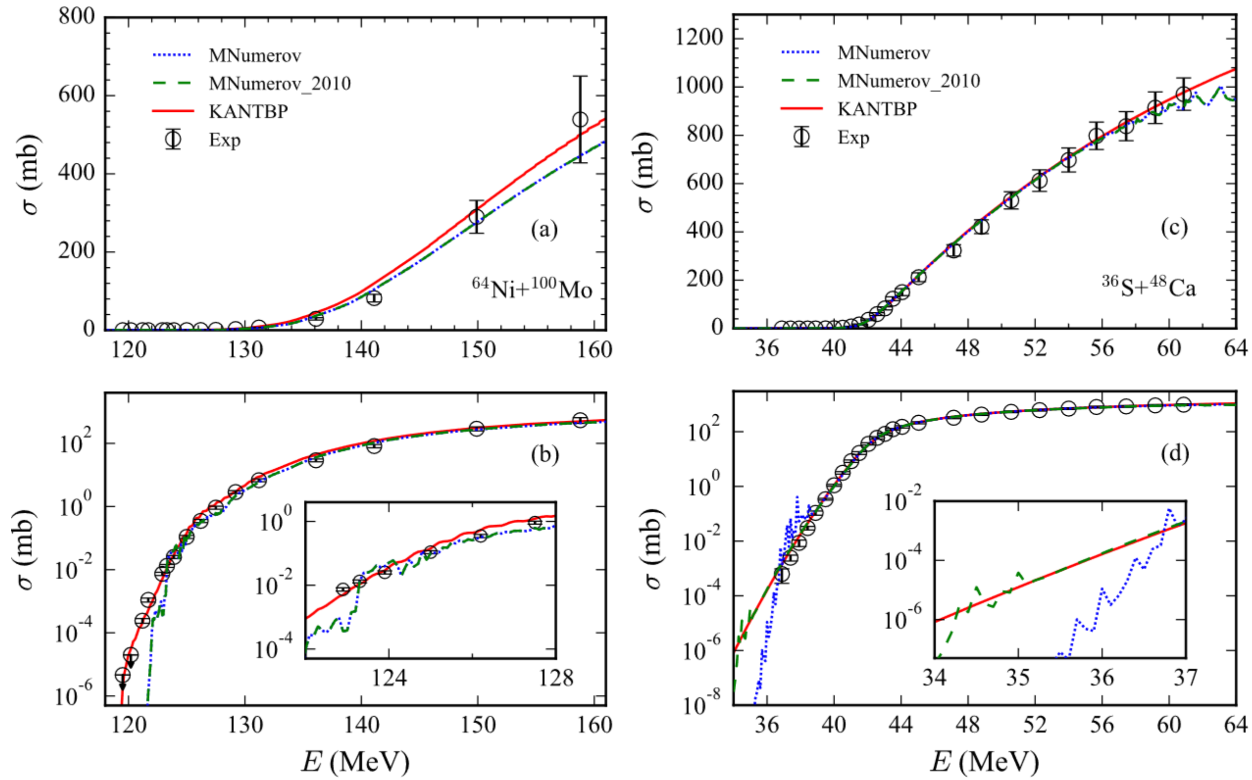

Fusion cross sections for ^{64}Ni+^{100}Mo ((a) in linear scale and (b) in logarithmic scale) and ^{36}S+^{48}Ca ((c) in linear scale and (d) in logarithmic scale). The experimental data (open circles) from Ref. [C.L. Jiang, et al, Phys. Rev. C 71 (2005) 044613; A.M. Stefanini et al, Phys. Rev. C 78 (2008) 044607] are shown for reference. The calculations are performed with the Woods-Saxon potential derived from the commonly adopted Akyüz-Winther parameterization, and 26 coupled channels are considered in the calculations. The results are calculated by means of the modified Numerov (MNumerov) method in the program CCFULL [K. Hagino, et al, Comput. Phys. Commun. 123 (1999) 143–152.] (dotted line), the improved Numerov method (MNumerov_2010) in the latest version of the program CCFULL [K. Hagino (2010), www2.yukawa.kyoto-u.ac.jp/~kouichi.hagino/ccfull/ccfull.f.] (dashed line) and KANTBP (solid line).

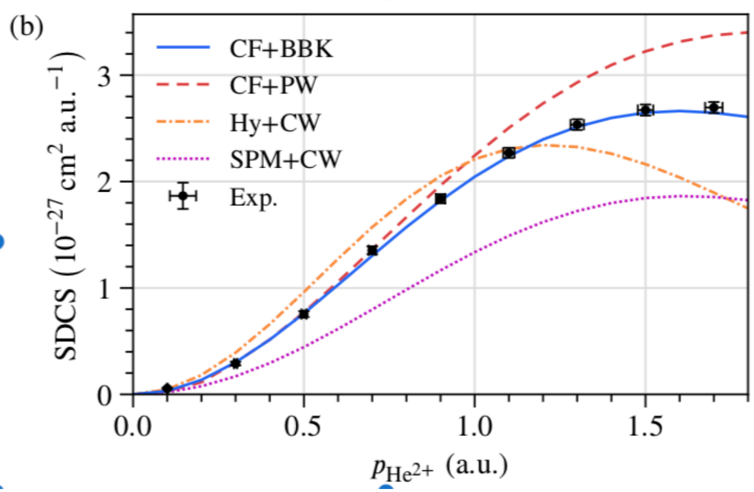

PHYSICAL REVIEW LETTERS 128, 053001 (2022)

Ion and Electron Momentum Distributions from Single and Double Ionization of Helium Induced by Compton Scattering

M. Kircher ,….., O. Chuluunbaatar, Yu. V. Popov, ….., R. Dörner.

Various cross sections of double Compton ionization of a helium atom by a photon with an energy of 40 KeV were measured using the COLTRIMS detector. The results were compared with theoretical calculations within the A^2 nonrelativistic approximation. For the first time, the momentum profile of the nucleus was experimentally obtained in this way.

Fig. ***Single differential cross section of double ionization of a helium atom vs nuclear momentum. Different curves correspond to pairs of initial and final trial wave functions with different degrees of electronic correlations.***

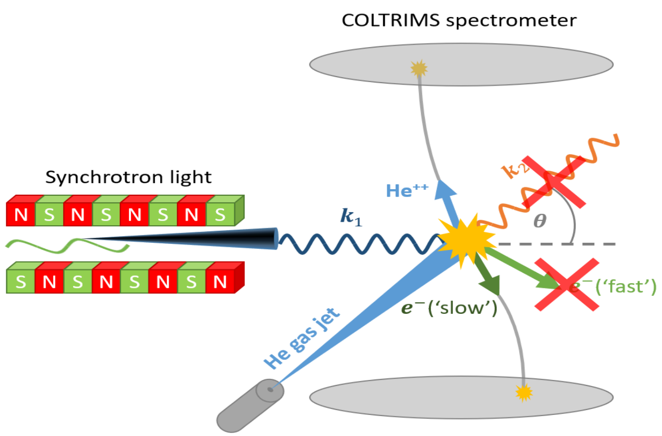

PHYSICAL REVIEW A **103**, 053109 (2021)

Improving efficiency of sympathetic cooling in atom-ion and atom-atom confined collisions

Vladimir S. Melezhik*

Bogoliubov Laboratory of Theoretical Physics, Joint Institute for Nuclear Research, Dubna, Moscow Region 141980, Russian Federation

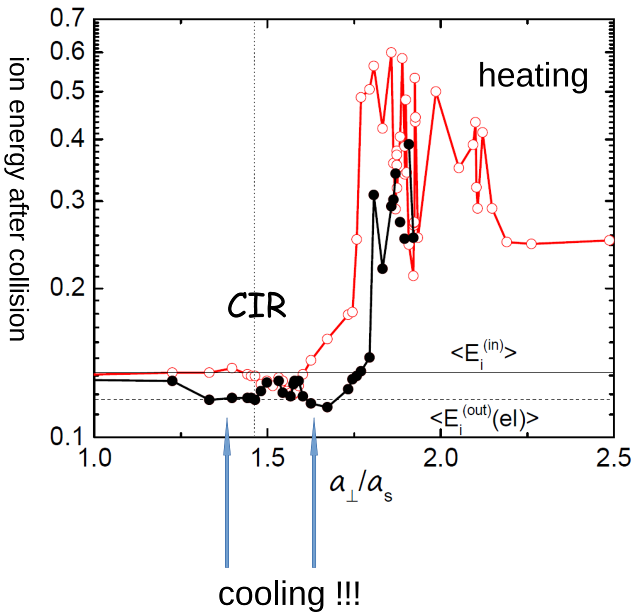

New mechanism for cooling ions in RF Paul traps:
to use buffer atoms near confinement-induced resonance (CIR)

It is shown: using CIR in atom-ion trap can resolve
long-standing problem of reaching quantum degeneracy of ions

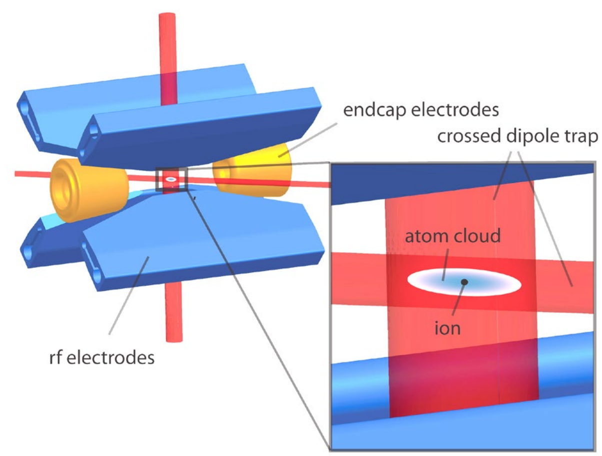

Project:

Relativistic nuclear dynamics and nonlinear quantum processes

S.Bondarenko, A.Larionov

A.I. Titov , U. Hernandes Acosta, B. Kampfer,
PRA 104,(2021), NJP 23,(2021),PRA,103(2021),
Eur.Phys.J.ST 230 (2021) 2445-2560

Further studying nonlinear, essentially multiphoton processes in quantum electrodynamics

Key process: positron distribution at largest emerging European laser project (XFEL, DESY)

LUXE-Collaboration (DESY) experiment

electron – laser set up

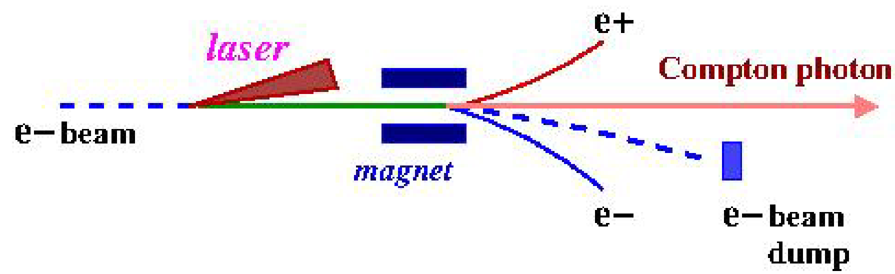

The e+e- pair production rate is expressed as a convolution nonlinear hard Compton photon production in e- laser interaction and nonlinear Breit-Wheeler e+e- production in γ– laser interaction. The number of laser photons involved in process may reach dozen thousand depending on laser field intensity

Non linear Compton high energy γ production $e + L \to \gamma + e'$	$\otimes$	Non linear Breit–Wheeler $e+\,e-$ pair production $\gamma + L \to e+ + e-$

Positron distribution in E144 (SLAC experiment (1997))

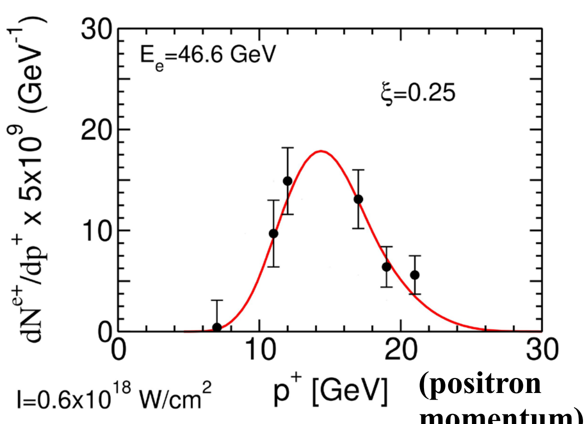

Predictions for LUXE experiment

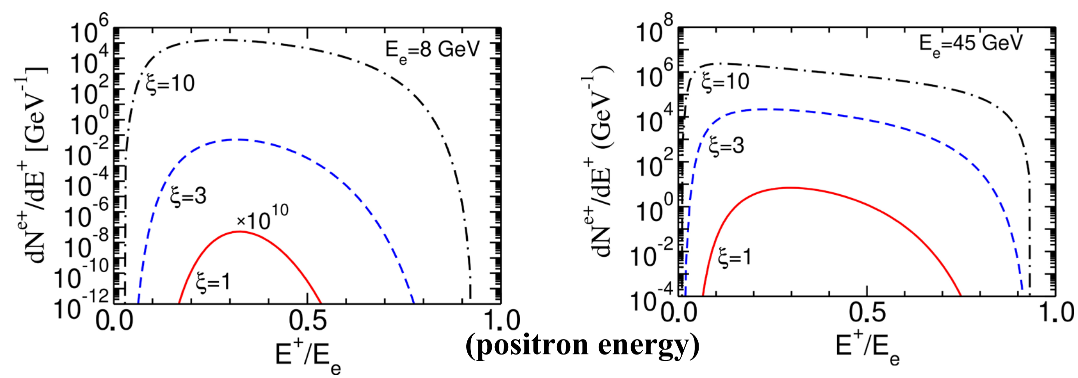

$for\ \xi = 1 - 10 \Rightarrow I_L \approx (4 - 400)\ 10^{18}\ \frac{W}{cm^2}$

ξ *is reduced field intensity* $\quad \xi^2 = \frac{0.56}{(\omega_L[\mathrm{eV}])^2} \times 10^{-18} I_L(\frac{\mathrm{W}}{\mathrm{cm}^2}),$ $\quad I_L$ *is the laser power*

Color coherence effects in the reaction d(p,2p)n

A.B. Larionov, Phys. Rev. C 107, 014605 (2023)

The color transparency (CT) phenomenon is the reduced interaction of the color neutral quark configurations – entering in or escaping from the hard interaction point – with surrounding nuclear medium. CT studies at intermediate energies (E_{beam} ~ 6-100 GeV) are already done or planned for a number of large-momentum-transfer ($Q^2 > 1$ GeV^2) reactions with nuclear targets:

JLab:

- A(e,e'π^+) – CT found for ^{12}C, ^{27}Al, ^{63}Cu, ^{197}Au
- A(e,e'ρ^0) – CT found for ^{12}C, ^{56}Fe
- A(e,e'p) – CT not found for ^{12}C, deuteron target planned

A($\bar{p}$,2π) - planned with deuteron target at FAIR PANDA

A(p,pp) - CT found (?) with Li, C, Al, Cu, Pb at BNL AGS, deuteron target planned at NICA SPD

The purpose of this work is to evaluate CT effects in the pd → ppn process where the incident proton and both outgoing protons are fast in the deuteron rest frame and can experience soft elastic rescattering by a slow neutron. CT influences the ISI/FSI of the protons. Calculations are done within the generalized eikonal approximation (GEA) based on the pole diagrams. The CT effects are introduced within the framework of the quantum diffusion model ***(G.R. Farrar, H. Liu, L.L. Frankfurt, M.I. Strikman, 1988)***. The nuclear transparency and the tensor analyzing power for the longitudinal deuteron polarization are calculated.

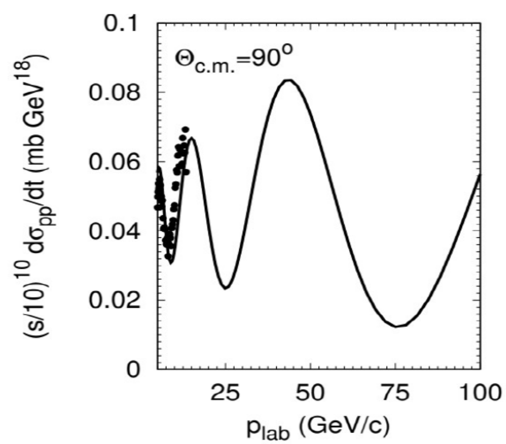

A.S. Parvan, ***Study of invariance of nonextensive statistics under the uniform energy spectrum translation***, **Physica A 588 (2022) 126556**

Motivation:

- In the high-energy physics community, it is generally considered that the Tsallis-1 statistics has a significant deficiency: it is not invariant under the uniform energy spectrum translation, $E_i' = E_i + E_0$
- The roots of this conviction go to the original papers of C. Tsallis.

Results:

➢ In the present paper, it was rigorously demonstrated that the Tsallis-1 statistics is invariant under the uniform energy spectrum translation.

➢ In addition, the invariance of the Tsallis-3 statistics and a non-invariance of the Tsallis-2 statistics under the total energy shift were confirmed.

➢ The invariance of the q-dual statistics (introduced by the author) under the uniform energy spectrum translation has also been proven.

S. Bondarenko, V. Burov and S. Yurev "Trinucleon form factors with relativistic multirank separable kernels", Nucl. Phys. A, 1014, 122251, 2021.

The **elastic electron-trinucleon scattering** in the relativistic impulse approximation is studied by using the **relativistic generalization of the Faddeev equations with a multirank separable kernel** of the nucleon-nucleon interactions.

- Static approximation (SA): without Lorentz boosts in the arguments of the propagators and vertex functions
- Relativistic corrections: with Lorentz boosts

^{3}H magnetic form factor with Graz-II kernel

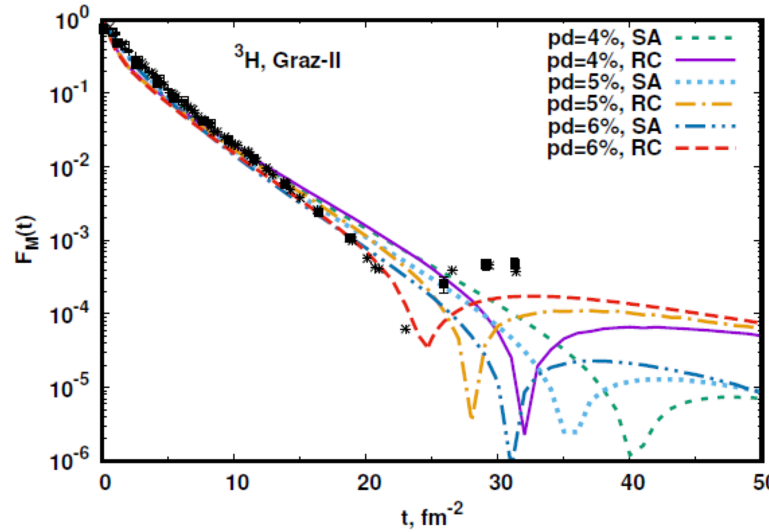

^{3}He magnetic form factor with Paris kernel

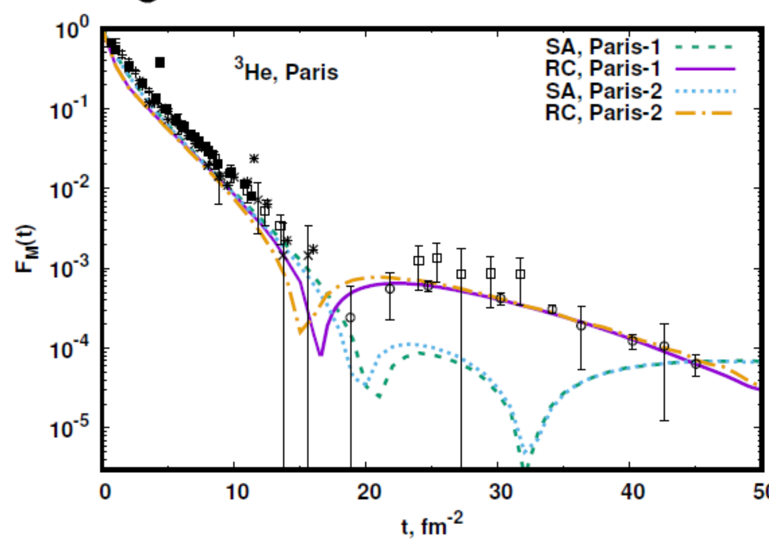

Mass spectrum of pseudo-scalar glueballs from a Dyson-Schwinger-Bethe-Salpeter approach.

L.P. Kaptari, B. Kaempfer, **Few Body Systems, 61, 28, 2020**

The masses of the ground and excited states of pseudo-scalar glueballs have been calculated within a framework based on the rainbow approximation to the Dyson-Schwinger and Bethe-Salpeter equations with effective parameters adjusted to lattice data. The partial BS amplitudes have been calculated as well.

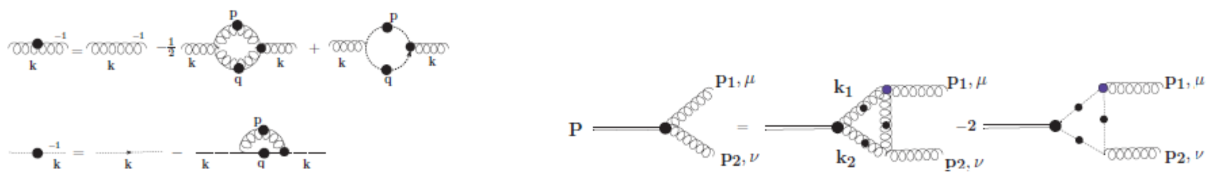

Dyson-Schwinger for gluon and ghost propagators (left panel); Bethe-Salpeter for glueballs (right panel)

RESULTS

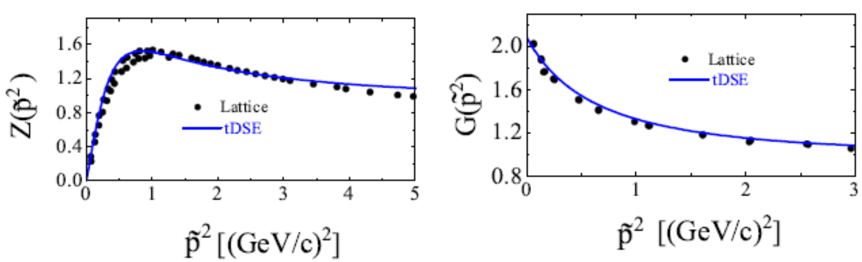

Solutions of the DS equations (solid lines) in comparison with lattice SU(2) calculations (filled circles). Left panel: gluon dressing function, right panel: ghost dressing function.

Agreements with theoretical groups from other institutes

BLTP – Germany (Heisenberg – Landau Program)	**since 1991**
BLTP – Romania (Titeica – Markov Program)	**since 2003**
BLTP – APCTP (Republic of Korea)	**since 2007**
BLTP – Bulgaria (Soloviev – Khristov Program)	**since 2009**
BLTP -- ITP CAS (China) **BLTP -- Egypt**	**since 2010** **since 2019**

Long-term cooperation with groups from France, Brazil, Hungary, India, Poland, Serbia, Belarus, Kazakhstan, Uzbekistan, South Africa, Sweden, Czech, UK, Moldova, Spain, and Russia

Cooperation with JINR Labs: FLNR, DLNP, MLIT, FLNP, LHEP

Concept of Theme «Theory of Nuclear Systems»

Development of theoretical methods ⟺ Applications for experiments

Multidisciplinar nature

Attraction of young researchers in nuclear theory

Our future theoretical studies will be closely related to the programs of operated and commissioning facilities at JINR (SHE-factory, ACCULINA-2) and in the world (FAIR, ISOL facilities HIE-ISOLDE, SPES, SPIRAL2, FRIB, RAON, HIAF). The studies of heavy-ion collisions at high energies will be related to the NICA project at JINR.